2nd URSI AT-RASC, Gran Canaria, 28 May – 1 June 2018

The impact of interplanetary shocks on whistler mode waves

Chao Yue[(1)], Jacob Bortnik[(1)], Hong Zhao*[(2)]
(1) Department of Atmospheric and Oceanic Sciences, University of California, Los Angeles, California, USA
(2) Laboratory for Atmospheric and Space Physics, University of Colorado Boulder, Boulder, CO, USA

Abstract

Magnetospheric whistler mode waves play a key role in regulating the dynamics of the electron radiation belts. Recent satellite observations indicate a significant influence of interplanetary (IP) shocks on whistler mode wave power in the inner magnetosphere. In this study, we statistically investigate the response of whistler mode chorus and plasmaspheric hiss to IP shocks based on Van Allen Probes and THEMIS satellite observations. Immediately after the IP shock arrival, chorus wave power is usually intensified, often at post-midnight to pre-noon sector, while plasmaspheric hiss wave power predominantly decreases near the dayside but intensifies near the nightside.

1. Introduction

Chorus emissions are intense electromagnetic whistler mode waves with discrete elements, excited naturally in the low-density region outside the plasmapause due to cyclotron instability of energetic anisotropic electrons [1, 2, 3]. They typically occur in the range 0.1–0.8 fce (fce is the equatorial electron cyclotron frequency), commonly in two distinct bands (lower and upper bands) with a gap near 0.5 fce [4]. Previous studies have shown that nightside chorus waves are confined to within ~15° of the magnetic equator, whereas dayside chorus waves can extend to higher magnetic latitudes (MLAT) [5, 6]. Recent studies have demonstrated the important role played by chorus waves in both the loss of plasma sheet electrons and the acceleration of radiation belt relativistic electrons [7, 8, 9].

Plasmaspheric hiss waves are structureless, broadband whistler mode emissions typically observed within the high plasma density regions that surround the Earth, including the plasmasphere and plasmaspheric plumes [10]. Plasmaspheric hiss is widely distributed in radial distance and magnetic local time (MLT); the strongest emissions typically occur in the dayside plasmasphere [11]. Plasmaspheric hiss causes precipitation of electrons from tens of keV to a few MeV to the upper atmosphere through pitch angle scattering on time scales ranging from days to weeks [12, 13]. Ray tracing and conjunctive satellite observations have shown that whistler mode chorus waves outside the plasmapause can propagate into the plasmasphere where they can be amplified further to form plasmaspheric hiss [14, 15, 16, 17]. Another possible mechanism of plasmaspheric hiss generation is excitation by the electron cyclotron instability in the outer plasmasphere [18].

The whistler wave power in the inner magnetosphere may significantly change following the arrival of an interplanetary (IP) shock. *Su et al.* [19] have reported enhanced damping and resultant disappearance of plasmaspheric hiss due to increased fluxes of superthermal electrons during an IP shock event with Van Allen Probes observations. The disappearance of plasmaspheric hiss and chorus waves may also be caused by increased field line inhomogeneity after the solar wind dynamic pressure decrease [20], which tends to inhibit wave growth and propagation.

Only Few studies of the whistler mode waves amplification/suppression have been done in the past due to the scarcity of such events and the fortuitous presence of near-Earth satellites at the right locations to observe the waves. It is thus presently unclear what the effects of IP shocks on whistler mode waves are as function of MLT, and what controls the wave amplification or damping during the passage of IP shocks. Such knowledge is critical to further understand the origin of particle acceleration or precipitation during the passage of IP shocks. Towards that goal, we surveyed 86 fast forward IP shock events from 2010 to 2016, which are identified as the abrupt increase of solar wind number density, temperature, velocity, magnetic field magnitude and dynamic pressure following the IP shock arrival, based on the upstream Advanced Composition Explorer (ACE) and Wind satellite observations (the shock list can be found here: https://www.cfa.harvard.edu/shocks/) to investigate the effects of IP shocks on the whistler mode waves, including plasmaspheric hiss and whistler mode chorus waves, using Van Allen Probes (A and B) and Time History of Events and Macroscale Interactions during Substorms (THEMIS) (A, D and E) spacecraft observations, and report the different responses of chorus wave and plasmaspheric hiss at different MLTs to the IP shocks. We used symH and AE indices as indicators of the shock arrival on the ground for consistency of all events, which may introduce a one or two minutes difference between our shock arrival time and the signal observed by the satellite in the magnetosphere. We also employed the two near-Earth ARTEMIS P1 and P2 satellites (also known as THEMIS B and C), when available, as high-fidelity upstream monitors.

2. Results

We investigate the wave power distribution of whistler mode waves during each of the 86 IP shocks. Seventy events were observed by Van Allen Probes and sixty by THEMIS, fewer due to THEMIS' higher apogee (~12R_E) causing those spacecraft to be located often outside the magnetopause after impact of the IP shock and also due to the ~50% duty cycle of high-resolution fast survey data due to telemetry limitations. The background electron density and/or upper hybrid resonance frequency are used to identify satellite location with respect to the plasmapause [21]. Plasmaspheric hiss waves are identified typically inside the plasmasphere, and chorus waves typically in the plasma trough. Each single spacecraft observation around any of the IP shocks is counted as one event. There are 123 events where spacecraft are inside the plasmasphere and 151 events where spacecraft are in plasma trough. Using 10^{-14} $(V/m)^2/Hz$ and 10^{-9} $(nT)^2/Hz$ as the lowest power thresholds for electric and magnetic power densities, respectively, we find 43 (35%) plasmaspheric hiss reduction/disappearance events, 36 (29%) plasmaspheric hiss excitation/intensification events and 62 (41%) chorus wave excitation/intensification events in response to the IP shocks, whereas no chorus wave disappearance event was found in this database. The rest of the events show either no wave activity or no wave intensity change, and we call them as non-wave events.

2.1. Case study

Opposite plasmaspheric hiss response were observed at different spacecraft located at different MLTs during a single IP shock event. Figure 1 shows an IP shock at 17:05 on 7 February 2014. THEMIS-C at (-8.3, 60.7, -2.8) R_E observed an IP shock at 17:04 UT as a total magnetic field (black curve) increase (5 to ~12nT), solar wind velocity (red curve) increase (-300 to -400 km/s), ion number density increase (4 to 13 cm^{-3}), and dynamic pressure increase (1 to 3 nPa) (Figure 1a). At 07:05 UT, AE and symH abruptly increased (0 to >150 nT and -5 to +20 nT, respectively) indicating the arrival of the shock. Shortly thereafter, THEMIS-D, at L=8.4 at dusk, observed newly excited chorus waves (Figure 1b), while Van Allen Probes A and B, both inside the plasmasphere, observed hiss intensification at dusk (Figure 1c) and hiss disappearance/reduction at pre-noon (Figure 1d), respectively. The suprathermal electron energy flux of 0.3 to 1 keV (Figure 1d) shows obvious increase following the IP shock arrival.

2.2. Statistical results

The representative observations in Figures 1 indicate that the chorus waves and plasmaspheric hiss can exhibit dramatically different responses to IP shocks, at different locations. To understand the characteristics of these whistler mode waves and look for patterns on a global scale, we have conducted a statistical survey by investigating the wave power variations during each of the 86 IP shock events we have identified. Figure 2 shows the statistical distributions of the whistler mode chorus and plasmaspheric hiss wave responses to IP shocks observed by the Van Allen Probes and THEMIS.

Van Allen Probes (cross signs) and THEMIS (diamond signs) locations at the time of IP shock arrival are shown in Figure 2a and 2d, together with the corresponding whistler wave response and non-wave events (color-coded). The rest of the bar plots show distributions of whistler events and non-wave events as function of MLTs and MLAT, respectively. Blue color represents hiss wave power reduction/disappearance; Red color represents hiss wave power intensification/excitation; Black represents chorus wave intensification/excitation; Green represents non-wave events. As seen in the Figure 2, there was only intensification and no evidence of chorus wave reduction from our IP shock event list (we only investigate the fast forward IP shock events in association with solar wind dynamic pressure increase).

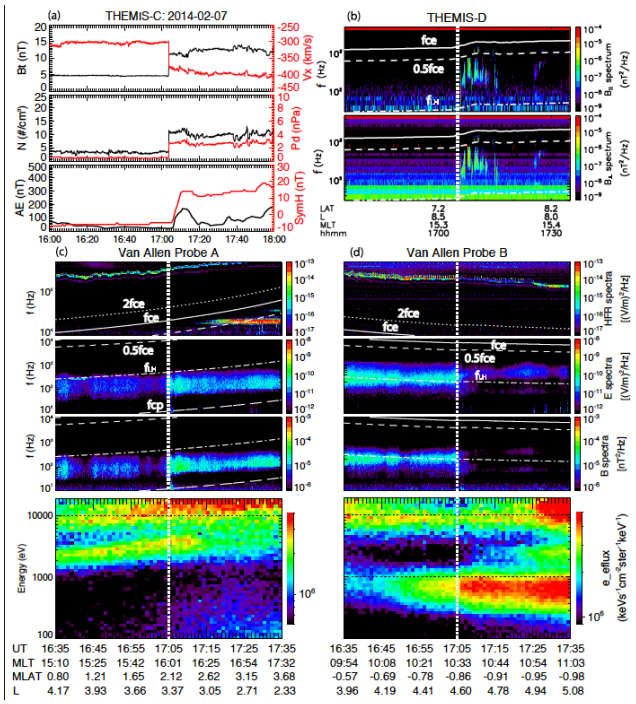

Figure 1. (a) An IP shock observed by the THEMIS-C spacecraft at 17:04 UT at (-8.3, 60.7, -2.8) RE in solar wind on 7 February 2014. The first panel shows magnetic field magnitude in black and the X-component of solar wind velocity in GSE coordinates in red. The second panel shows ion density in black and dynamic pressure in red. The bottom panel shows the variations of AE index in black and symH in red. (b) The magnetic field power spectral density in the parallel and perpendicular directions observed by THEMIS-D. The vertical dashed line marks the IP shock arrival time. (c) and (d) are the wave and electron measurements made by Van Allen Probes A and B, respectively. The panels from top to bottom are the electric spectral density in the HFR channel, electric and magnetic field power spectral density in the WFR channel, and the omni-directional electron energy flux from 0.1 to 20 keV. The vertical dashed line marks the shock arrival time.

Chorus wave amplifications are mostly observed at higher L shells and outside the plasmasphere (Figure

2a), with a higher occurrence rate of chorus intensification near the post-midnight to pre-noon sectors when compared with the dusk sector as shown in Figures 2b and 2g. This is mainly caused by the eastward drift of electrons injected from the tail plasma sheet, providing the free energy source for the excitation of chorus waves. On the other hand, non-chorus wave events are mainly located on the nightside at large L shell, which is probably related to the satellite orbits. In contrast, the plasmaspheric hiss wave disappearance/reduction occurs mostly on the dayside with peak occurrence around noon reaching about 70% (Figures 2d, 2e and 2h), while the hiss intensification events occur at all local times with higher occurrence rate on the nightside (Figures 2d, 2e and 2i) following the IP shocks arrival. In addition, the non-hiss wave events predominantly occur on the nightside compared with the number of events on the dayside (Figures 2d and 2e). The immediate reduction/disappearance of plasmaspheric hiss following the IP shock arrival, demonstrates that hiss damping rates should be significantly increased, such that hiss wave lifetimes is comparable to the short time scale of the shock impact (~1 min). Although more wave events were observed in general at lower latitude ranges (due to the spacecraft trajectory), no clear latitude dependence of the whistler mode wave response is found in our survey as demonstrated in Figure 2c and 2f.

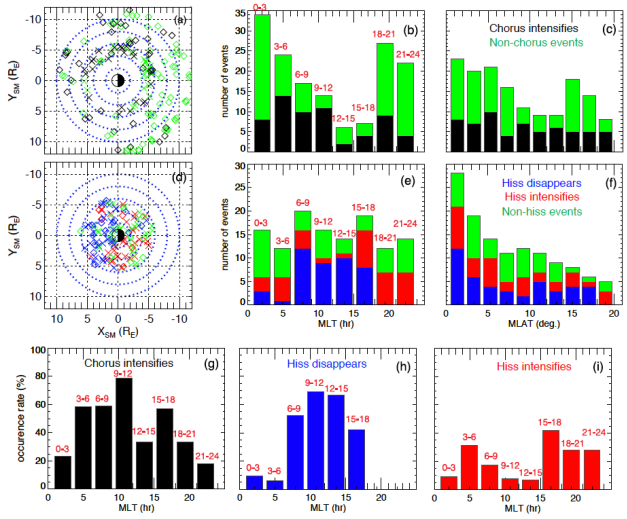

Figure 2. The global distribution of the whistler mode chorus and plasmaspheric hiss wave responses to IP shocks observed by Van Allen Probes and THEMIS satellites. (a) and (d): Distribution in the X-Y plane in SM coordinates outside the plasmasphere (a) and inside the plasmasphere (d). The cross sign represents the locations of Van Allen Probes and the diamond sign represents the locations of THEMIS satellites around the IP shock arrival time; (b) /(e) and (c)/(f): Chorus/hiss event distributions as function of MLTs (b)/(e) and MLAT (c)/(f). Black represents chorus wave intensification/excitation (g)-(i) Occurrence rate as a function of MLTs: (g) Chorus intensification/excitation events; (h) Hiss reduction/disappearance events; (i) Hiss intensification/excitation events. Blue color represents hiss wave reduction/disappearance; Red color represents hiss wave intensification/excitation; Black represents chorus wave intensification/excitation; Green color represents non-wave events.

3. Summary and Conclusions

In this paper, we have performed a statistical study of whistler mode wave modifications in response to IP shocks based on data from both Van Allen Probes and THEMIS observations. 86 IP shock events were studied and we found 43 (35%) plasmaspheric hiss reduction/disappearance events, 36 (29%) hiss excitation/intensification events and 62 (41%) chorus wave excitation/intensification events from single satellite observation. Our main findings are:

1. Chorus wave power is usually intensified, with most cases occurring predominately at post-midnight to pre-noon sector.
2. Plasmaspheric hiss disappearance events occur predominantly on the dayside while plasmaspheric hiss intensifications occur mostly on the nightside.

On average, plasmaspheric hiss intensities are an order of magnitude larger on the dayside than on the nightside due to stronger Landau damping on the nightside, and hiss intensity increases during high solar wind dynamic pressure [22]. However, in this study, we have demonstrated that abrupt solar wind dynamic pressure increases cause plasmaspheric hiss disappearance on the dayside and intensification on the nightside. The MLT-dependent response of plasmaspheric hiss to IP shocks was not expected and is not well understood. For example, Landau damping could be a factor causing the hiss reduction/disappearance on the dayside. Since the wave power and distributions significantly vary following the IP shock arrival, our study suggests the importance of investigating the detailed wave and particle distributions in studying the local wave-particle interactions especially around the periods of IP shocks.

4. Acknowledgements

We acknowledge use of Van Allen Probes data of the Level 3 HOPE omni-dimensional data obtained from the RBSP-ECT website, made publicly available through NASA prime contract number NAS5-01072. We acknowledge the Van Allen Probes data from the EMFISIS and the THEMIS data. We thank the World Data Center for Geomagnetism, Kyoto for providing geomagnetic indices and the Space Physics Data Facility at the NASA Goddard Space Flight Center for providing the OMNI data.

5. References

1. Meredith, N. P., R. B. Horne, R. M. Thorne, and R. R. Anderson (2003), Favored regions for chorus-driven electron acceleration to relativistic energies in the Earth's outer radiation belt, Geophys. Res. Lett., 30(16),1871, doi:10.1029/2003GL017698.

2. Yue, C., X. An, J. Bortnik, Q. Ma, W. Li, R. M. Thorne, G. D. Reeves, M. Gkioulidou, D. G. Mitchell, and C. A. Kletzing (2016b), The relationship between the macroscopic state of electrons and the properties of chorus waves observed by the Van Allen Probes, Geophys. Res. Lett., 43, 7804–7812, doi:10.1002/2016GL070084.
3. An, X., C. Yue, J. Bortnik, V. Decyk, W. Li, and R. M. Thorne (2017), On the parameter dependence of the whistler anisotropy instability, J. Geophys. Res. Space Physics, 122, doi:10.1002/2017JA023895.
4. Santolík, O., D. A. Gurnett, J. S. Pickett, M. Parrot, and N. Cornilleau-Wehrlin (2003), Spatio-temporal structure of storm-time chorus, J. Geophys. Res., 108(A7), 1278, doi:10.1029/2002JA009791.
5. Li, W., Thorne, R.M., Angelopoulos, V., Bortnik, J., Cully, C.M., Ni, B., LeContel, O., Roux, A., Auster, U. and Magnes, W. (2009), Global distribution of whistler-mode chorus waves observed on the THEMIS spacecraft, Geophys. Res. Lett., 36, L09104, doi:10.1029/2009GL037595.
6. Bunch, N. L., M. Spasojevic, and Y. Y. Shprits (2011), On the latitudinal extent of chorus emissions as observed by the Polar Plasma Wave Instrument, J. Geophys. Res., 116, A04204, doi:10.1029/2010JA016181.
7. Horne, R. B., Thorne, R.M., Shprits, Y.Y. and Meredith, N.P. (2005), Wave acceleration of electrons in the Van Allen radiation belts, Nature, 437, 227–230, doi:10.1038/nature03939.
8. Li, W., Y. Y. Shprits, and R. M. Thorne (2007), Dynamic evolution of energetic outer zone electrons due to wave-particle interactions during storms, J. Geophys. Res., 112, A10220, doi:10.1029/2007JA012368.
9. Thorne, R. M., Li, W., Ni, B., Ma, Q., Bortnik, J., Baker, D.N., Spence, H.E., Reeves, G.D., Henderson, M.G., Kletzing, C.A. and Kurth, W.S. (2013), Evolution and slow decay of an unusual narrow ring of relativistic electrons near L ~ 3.2 following the September 2012 magnetic storm, Geophys. Res. Lett., 40, 3507–3511, doi:10.1002/grl.50627.
10. Summers, D., B. Ni, N. P. Meredith, R. B. Horne, R. M. Thorne, M. B. Moldwin, and R. R. Anderson (2008), Electron scattering by whistler-mode elf hiss in plasmaspheric plumes, J. Geophys. Res., 113, A04219, doi:10.1029/2007JA012678.
11. Li, W., Q. Ma, R. M. Thorne, J. Bortnik, C. A. Kletzing, W. S. Kurth, G. B. Hospodarsky, and Y. Nishimura (2015), Statistical properties of plasmaspheric hiss derived from Van Allen Probes data and their effects on radiation belt electron dynamics, J. Geophys. Res. Space Physics, 120, 3393–3405, doi:10.1002/2015JA021048.
12. Meredith, N. P., R. B. Horne, S. A. Glauert, D. N. Baker, S. G. Kanekal, and J. M. Albert (2009), Relativistic electron loss timescales in the slot region, J. Geophys. Res., 114, A03222, doi:10.1029/2008JA013889.
13. Ma, Q., Li, W., Thorne, R.M., Bortnik, J., Reeves, G.D., Kletzing, C.A., Kurth, W.S., Hospodarsky, G.B., Spence, H.E., Baker, D.N. and Blake, J.B (2016), Characteristic energy range of electron scattering due to plasmaspheric hiss, J. Geophys. Res. Space Physics, 121, 11, 737–11, 749, doi:10.1002/2016JA023311.
14. Bortnik, J., R. M. Thorne, and N. P. Meredith (2008), The unexpected origin of plasmaspheric hiss from discrete chorus emissions, Nature, 452, 62–66, doi:10.1038/nature06741.
15. Bortnik, J., W. Li, R. M. Thorne, V. Angelopoulos, C. Cully, J. Bonnell, O. LeContel, and A. Roux (2009a), An observation linking the origin of plasmaspheric hiss to discrete chorus emissions, Science, 324, 775–778.
16. Bortnik, J., R. M. Thorne, and N. P. Meredith (2009b), Plasmaspheric hiss overview and relation to chorus, J. Atmos. Sol. Terr. Phys., 71, 1636–1646.
17. Chen, L., J. Bortnik, W. Li, R. M. Thorne, and R. B. Horne (2012), Modeling the properties of plasmaspheric hiss: 1. Dependence on chorus wave emission, J. Geophys. Res., 117, A05201, doi:10.1029/2011JA017201.
18. Thorne, R. M., S. R. Church, and D. J. Gorney (1979), On the origin of plasmaspheric hiss: The importance of wave propagation and the plasmapause, J. Geophys. Res., 84, 5241–5247, doi:10.1029/JA084iA09p05241.
19. Su, Z., Zhu, H., Xiao, F., Zheng, H., Wang, Y., Shen, C., Zhang, M., Wang, S., Kletzing, C.A., Kurth, W.S. and Hospodarsky, G.B. (2015), Disappearance of plasmaspheric hiss following interplanetary shock, Geophys. Res. Lett., 42, 3129–3140, doi:10.1002/2015GL063906.
20. Liu, N., Su, Z., Gao, Z., Zheng, H., Wang, Y., Wang, S., Spence, H.E., Reeves, G.D., Baker, D.N., Blake, J.B. and Funsten, H.O. (2017), Simultaneous disappearances of plasmaspheric hiss, exohiss, and chorus waves triggered by a sudden decrease in solar wind dynamic pressure, Geophys. Res. Lett., 44, 52–61, doi:10.1002/2016GL071987.
21. Meredith, N. P., R. B. Horne, R. M. Thorne, D. Summers, and R. R. Anderson (2004), Substorm dependence of plasmaspheric hiss, J. Geophys. Res., 109, A06209, doi:10.1029/2004JA010387.
22. Tsurutani, B. T., B. J. Falkowski, J. S. Pickett, O. Santolik, and G. S. Lakhina (2015), Plasmaspheric hiss properties: Observations from Polar, J. Geophys. Res. Space Physics, 120, 414–431, doi:10.1002/2014JA020518.